Motility of Bile Canaliculi in the Living Animal: Implications for Bile Flow

Norihito Watanabe, Nobuhiro Tsukada, Charles R. Smith, and M. James Phillips

Research Institute and Departments of Pathology and Pediatrics, The Hospital for Sick Children and University of Toronto, Toronto, Ontario, Canada M5G 1X8

Abstract. Modern fluorescence microscopic techniques were used to image the bile canalicular system in the intact rat liver, in vivo. By combining the use of sodium fluorescein secretion into bile, with digitally enhanced fluorescence microscopy and time-lapse video, it was possible to capture and record the canalicular motility events that accompany the secretion of bile in life. Active bile canalicular contractions were found predominantly in zone 1 (periportal) hepatocytes of the liver. The contractile movements were repetitive, forceful, and appeared unidirectional moving bile in a direction towards the portal bile ducts. Contractions were not seen in the network of canaliculi on the surface of the liver. Cytochalasin B administration resulted in reduced canalicular motility, progressive dilation of zone 1 canaliculi, and impairment of bile flow. Canalicular dilations invariably involved the branch points of the canalicular network. The findings add substantively to previous in vitro studies using couplets, and suggest that canalicular contractions contribute physiologically to bile flow in the liver.

ACTIN, myosin and associated proteins involved in contractile movements have been found in smooth muscle and nonmuscle cells (1, 16, 18, 24, 42, 43, 56, 61, 65). The majority of motility studies have been in vitro because this allows careful analysis of movements and of factors that influence them (23, 26, 27, 43, 46, 59, 64, 68). It has been difficult to study the fine details of cell motility in vivo because of technical limitations in resolution, but the marriage of computer-based, digital image processing with conventional microscopy achieves significant improvements in resolution, contrast, and visibility of fine detail. Most reports using these techniques used single cells or flattened cells or their processes (2, 3, 4, 26, 27, 38). Here we report on the use of fluorescence imaging to demonstrate bile canalicular contractions in the substance of the liver, in the living state.

Bile canaliculi are small channels formed by modifications of the plasma membranes of adjacent hepatocytes. Under normal conditions they are not visualized by conventional light microscopy. It is into these fine canals that bile is secreted by the liver cells. It has been generally considered that these are rigid channels that lack motility and that function as mere conduits conveying bile to the portal bile ducts. However, the bile canaliculi are surrounded by a rich investment of actin filaments (20, 21, 28, 29, 33, 34, 39, 40, 50, 53). Using isolated hepatocyte couplets and time lapse microscopy, it has been shown that bile canaliculi repeatedly open and close and that this motion is accompanied by the expelling of a bolus of bile (52, 55). We have interpreted this motility as active bile canalicular contractions (47, 52, 54, 55, 66), but others consider the motile events as noncontractile collapses of canaliculi resulting from secretory pressure with rupture of canaliculi (9, 11, 30, 35). In this report, we have taken advantage of the biliary secretion of sodium fluorescein by hepatocytes to visualize the bile canalicular system and have examined canalicular motility in the living state in order to shed light on these issues. These experiments which visualize the canalicular apparatus using sodium fluorescein, represent one of the few successful applications of modern fluorescence techniques to whole tissues.

Materials and Methods

Normal Rat Liver

Female Wistar strain rats weighing 140–160 g and fed laboratory rat diet and tap water ad libitum were used. The rats were anesthetized by intraperitoneal injection of sodium pentobarbital (50 mg/kg rat body weight). A lower midline abdominal incision allowed access to the ileocecal region and a large and straight mesenteric vein was cannulated with a polyethylene tube (PE10). After closing the abdomen, an incision was made in the upper abdominal midline and along the right costal margin. The edge portion of the middle liver lobe was gently placed on the glass portion of a microscope stage specially designed for the rat (51). A physiological state was maintained by wrapping the middle liver lobe in a plastic film, using a 38°C temperature controlled room. A solution of 0.3 ml of 1% sodium fluorescein (Uranin; Fisher Scientific Co. (Pittsburgh, PA) in physiological saline was rapidly administered via the mesenteric venous catheter.

Cytochalasin Infusion

In addition to the above preparation, the common bile duct was cannulated with polyethylene tubing (PE50) to measure bile flow. This catheter was inserted into the proximal one-third of the common bile duct to avoid contam-

ination with pancreatic juice (53). Cytochalasin B (CB)[1] solution was prepared from a stock solution consisting of 10 mg/ml of CB dissolved in DMSO, and then added to 3 mM PBS (pH 7.4) containing 10% BSA (Sigma Chemical Co., St. Louis, MO) (49, 53). The liver was infused with CB via the mesenteric venous catheter (PE10) at the rate of 3.3 μg/min/100 g body weight for 2 h, after which this infusion was stopped. Livers in control animals were infused with the same DMSO solution but without CB.

Brief Technical Comment on the uses of Sodium Fluorescein and CB in these Experiments

(*a*) Sodium fluorescein, which is commonly used for studying physiologic functions of tissues, is excreted into bile canaliculi (7, 36) and into urine (19) following systemic administration. Hanzon reported that sodium fluorescein is concentrated ~500 times in bile, and the biliary excretion of this dye is characterized as an active transport process (36). In vitro studies revealed that this dye is taken up by hepatocytes and excreted into bile across the bile canalicular membrane (5, 31). In this work, fluorescein was used as a probe to visualize the canalicular system, but since it is secreted into bile, it was also used to measure bile flow.

(*b*) The effects of the cytochalasins have been extensively studied, including their alteration of the structure and function of actin filaments and their striking effects on motility (63, 69). The mechanism by which they act on actin filaments is neither simple nor fully understood (12–15, 17, 25, 32, 37, 44, 45, 51, 60). One suggestion is that if they release the filaments from capping proteins, the filaments may contract into foci (17), which may explain the granular appearance seen by EM. In liver cells, CB also induces loss of membrane-associated Mg^{2+}-ATPase, and ruthenium red surface coat of bile canaliculi (49). It is unlikely that the CB effects described in this report are attributable to inhibition of hexose transport across the membrane (48) since impaired bile flow has also been found with cytochalasin D (personal observations) which has no effect on hexose transport (57).

Digitally-enhanced Fluorescent Imaging

The liver edge was observed through an inverted microscope (Diaphot TMD-EF; Nikon Inc., Garden City, NY) using digitally enhanced fluorescence imaging (3, 4, 26). Two microscope modes were used. One mode consisted of epifluorescence with 20 and 40× fluorescence objectives and a 100× glycerin objective, a B1 filter cassette (exciting filter 420–485 nm, dichroic mirror DM510 nm, absorption filter 520–560 nm), ultraviolet cutting, and neutral density filters, and a high pressure mercury lamp. The same field of the liver edge was also observed in a second mode by means of transillumination with the same objectives. The combination of CB infusion and major surgery results in a high mortality in rats. Reliable results of the liver changes could however, be obtained in stabilized animals 2 h after CB infusion. The observations in the CB group were made 2 h after its administration.

An extremely low level of illumination was used to minimize damage from photooxidation of the fluorophore and from any residual, unfiltered UV light. The weak fluorescent images were captured with a silicon intensified target (SIT) camera (C1000-12; Hamamatsu Corp., Bridgewater, MA) which had been modified to allow user control of the gain and bias characteristics of the camera tube. Signal output was in the form of a 512 × 512 pixel image (256 gray scale) which was routed to a video frame processor (C1440; Hamamatsu) to improve the signal-to-noise ratio by means of video frame averaging, giving a running average of 50 frames at a generation rate of 30 frames per second. The video signal was transferred to a time-lapse video cassette recorder (Panasonic NV8050).

Image Analysis Quantitation

Measurement of canalicular activity was based upon changes in the intensity of fluorescence in the segments of bile canaliculi seen in the captured video sequences. Using an image analyzer (Perceptics, Knoxville, TN) based on a computer (Macintosh IICX; Apple Computer, Cupertino, CA), a rectangle was drawn around each segment of the bile canalicular apparatus, and the integrated optical density (IOD) of each of these areas was obtained. To control for variations in illumination and other internal factors affecting the intensity of the image as a whole (e.g., light leaks into the darkened room where the experiment was performed), the IOD of the entire field of rat liver was also obtained for use as a correction factor.

1. *Abbreviations used in this paper*: CB, cytochalasin B; IOD, integrated optical density; SIT, silicon intensified target.

Measurement of Bile Flow

Bile was collected every 30 min before injection of sodium fluorescein and every 15 min for up to 60 min after the injection in the CB-infused and control groups. Bile flow was determined by weighing the collected bile in a preweighed tube. The time between the injection and the appearance of sodium fluorescein in bile was estimated to examine the effect of CB on the excretion of sodium fluorescein into bile. The concentration of sodium fluorescein in bile was measured using a fluorescence spectrophotometer (Perkin Elmer LS-5; Oak Brook Instrument Division, IL) whose excitation and emission were set to 494 and 517 nm, respectively. The pH of the bile in each of the samples collected was determined using a pH meter with flat-surface electrode (Fisher Scientific), in both control and CB-treated animals.

Procedure for EM

The rat livers of CB-infused and the control groups were fixed after the 2 h infusion of CB or albumin solution containing DMSO. The liver was perfused via the portal vein cannula with 1.2% glutaraldehyde buffered with 0.05 M sodium cacodylate solution (pH 7.4) containing 50 mM lysine (11) at 40 cm H_2O of perfusion pressure. For scanning EM, the well perfused areas were cut into small blocks (~1 × 1 × 5 mm^3) and postfixed with 2% osmium tetroxide in 0.1 M cacodylate buffer for 3 h at 4°C, followed by dehydration in a graded series of ethanol solutions. The tissue blocks were then fractured using a pair of forceps and prepared with a critical point dryer (E3100 Jumbo Series II; Polaron Equipment, Watford, England). After gold coating using a cold sputter etch unit (DESK-1; Denton Vacuum, Cherry Hill, NJ), the fractured surfaces of liver tissues were examined in a scanning electron microscope (JSM-335, JEOL, Tokyo, Japan) with 20 kV acceleration voltage. For transmission EM, the tissues were fixed by the perfusion technique as described above, and cut into small blocks (1 × 1 mm^3), followed by postfixation with 1% osmium tetroxide for 2 h at 4°C. Some tissue blocks were stained with 1% uranyl acetate in aqueous solution for 1 h at room temperature before dehydration (49, 50) in a graded series of ethanol and embedding in Epon-Araldite. Ultrathin sections were cut with a diamond knife on an Ultramicrotome (LKB2088 Ultratome V; LKB Produkter AB, Stockholm, Sweden) and stained in saturated aqueous uranyl acetate solution and Sato's lead solution (58). The specimens were examined in a transmission electron microscope (model EM400; Philips Electronic Instruments, Inc., Mahwah, NJ) with 60 kV acceleration voltage.

Results

Normal Rat Liver

The dynamic intraparenchymal blood flow beneath the surface of the rat liver was observed. The blood flowed radially from the terminal portal venules into the sinusoids surrounding the portal tracts. The sinusoidal blood flow was uniform and rapid, draining into the terminal hepatic venules. Approximately 2–3 s after the injection of sodium fluorescein, fluorescence microscopy revealed a yellow fluorescence filling the sinusoids adjacent to the terminal portal venules (Fig. 1 *a*). The fluorescein was distributed evenly to the sinusoids from the terminal portal venules and immediately disappeared into the terminal hepatic venules (Fig. 1 *b*). 20–30 s later, the liver parenchyma began to fluoresce (Fig. 1 *c*); this persisted for ~30 min. The subsequent decrease in hepatocyte fluorescence coincided with the appearance of the fluorescein in the bile canaliculi.

Although the images obtained directly from the camera were uninterpretable, with real time image processing the fluorescence of bile canaliculi was clearly recognizable and for up to 120 min (Figs. 2, *a–f*). A polygonal, two-dimensional meshwork of bile canalicular fluorescence was seen when the focus of the microscope was adjusted to visualize the superficial cell lamina on the surface of the liver (Fig. 2 *d*). By focusing deeper, bile canaliculi forming a three-

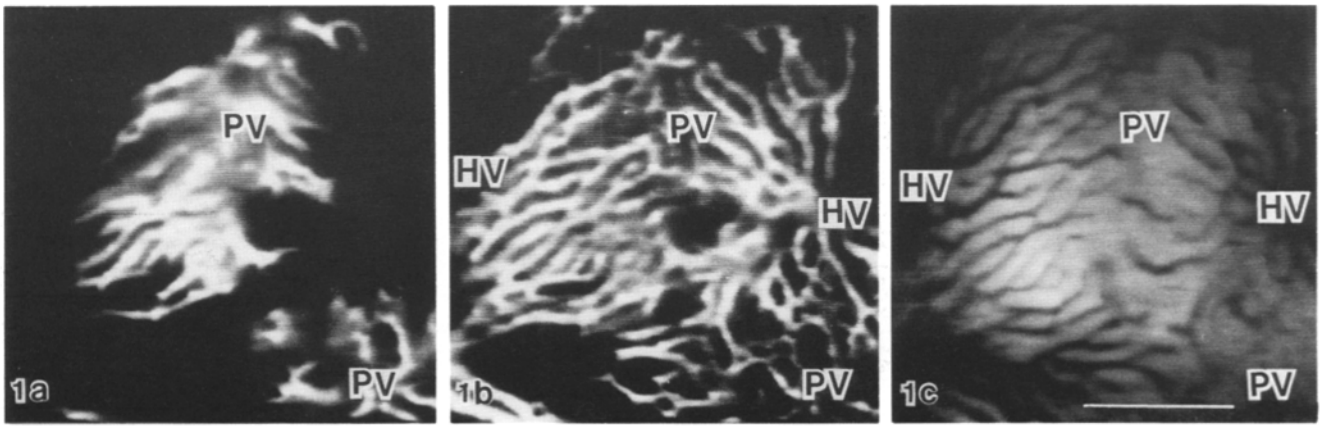

Figure 1. Fluorescent cinephotomicrographs of a portion of the liver in vivo, showing the in vivo liver microcirculation after the injection of sodium fluorescein. In *a*, a brilliant yellow fluorescence appears in the part of the sinusoids adjacent to the terminal portal venules (*PV*). The fluorescence seen in *b* is evenly distributed to the sinusoids in a radial fashion from the terminal portal venules (*PV*), converging to the terminal hepatic venules (*HV*). In *c*, the fluorescence is no longer found in the sinusoids but the liver cell cords have bright fluorescence a short time later. Bar, 100 μm.

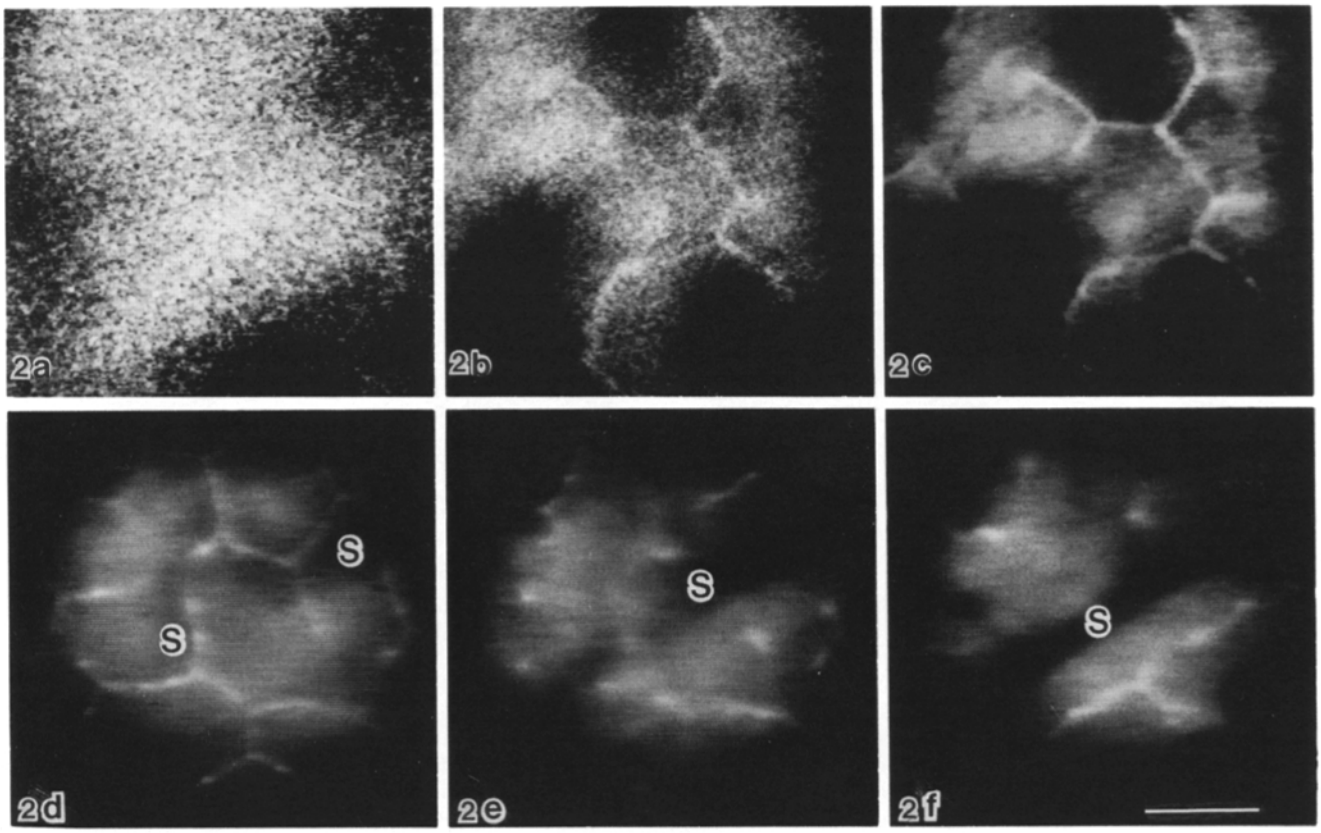

Figure 2. Comparison of results using digitally enhanced fluorescence imaging. *a* shows the imaging before capture by the SIT camera. Note that all that can be seen is "snow." *b* is the same image captured by the SIT camera and displayed on a monitor. The image is unprocessed. Bile canaliculi, albeit fuzzy, can now be recognized. *c* shows the same image using real-time image processing. Note the sharper definition of the bile canaliculus network (chicken-wire mesh appearance). (*d-f*) Fluorescent cinephotomicrographs ~60 min after the injection of sodium fluorescein. The fluorescence of the bile canaliculi is clearly recognized in the rat liver in vivo. (*S*) sinusoid. In *d*, a polygonal meshwork of the bile canalicular fluorescence is seen if the focus of the microscope is adjusted to visualize the superficial cell lamina on the surface of the liver. By focusing slightly deeper, the fluorescence pattern of bile canaliculi is changed in *e*. By focusing more deeply, the linear fluorescence pattern of bile canaliculi in the substance of the liver cell cords is well visualized in *f*. These two kinds of fluorescence pattern of bile canaliculi is found to be connected to each other by changing the focus of the microscope. Bar, 10 μm.

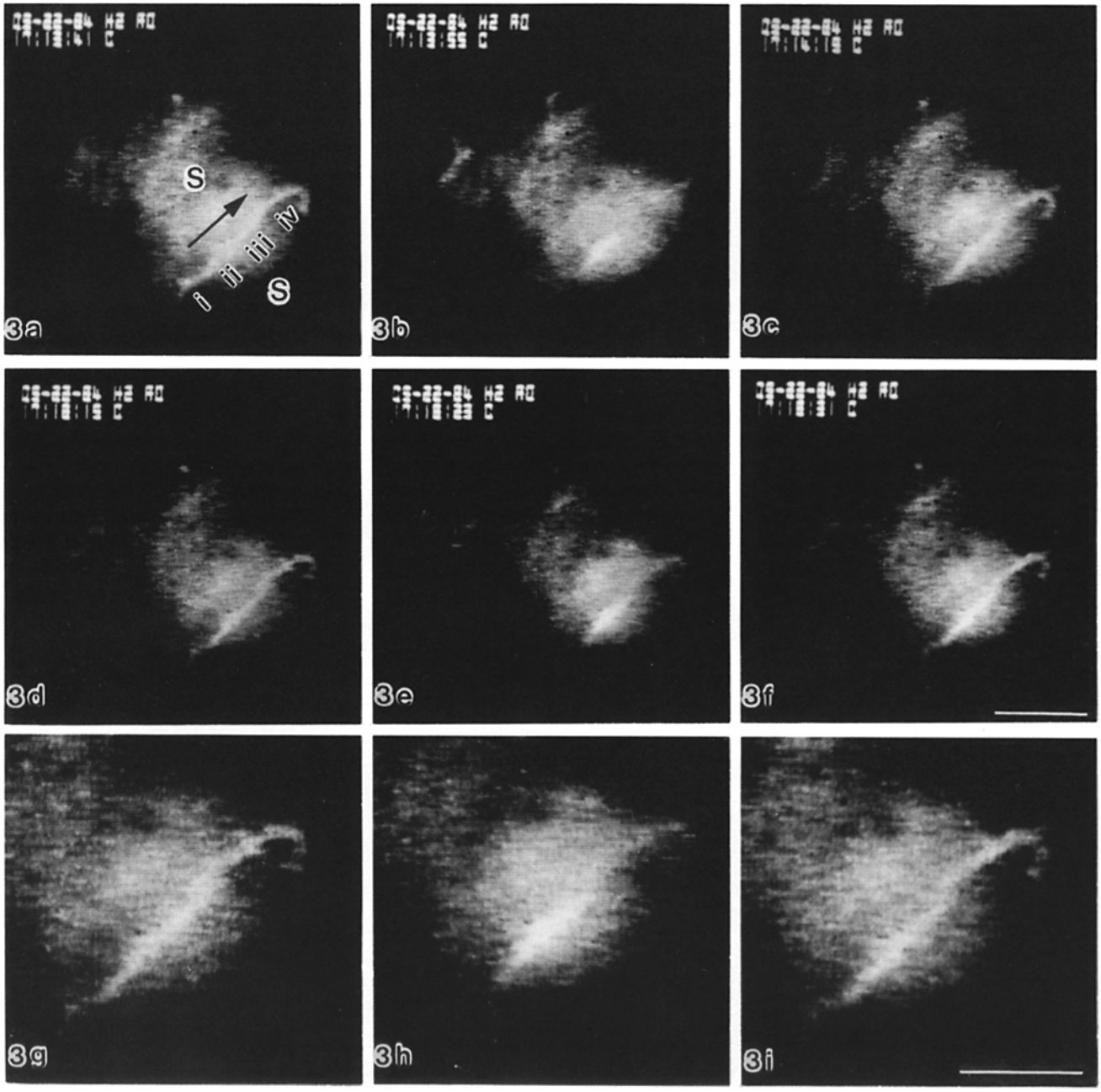

Figure 3. Fluorescent cinephotomicrographs show the sequence of bile canalicular contractions in vivo. The region illustrated is a portion of the canalicular network deep in the substance of the liver. A time-lapse series is shown with the real-time values in the upper left corner of each micrograph. The horizontal lines are rastral lines. The bile canalicular region imaged (white line with a hook) is outlined by sodium fluorescein which has been secreted into the canalicular lumen. The background staining of the cells remains virtually unchanged throughout, hence, there is no change in focus. The time for the completion of the contraction sequence in *a–c* is 17:14:19–17:13:41, i.e., 38 s. *d–f* show another contraction sequence of the same group of bile canaliculi as shown in *a–c*. In these micrographs, the pattern of the bile canalicular contractions is similar to that of *a–c*, but the contraction time is 16 s. In the canalicular region (*a–c*), four segments of approximately equal length can be identified: (*i*), lower end; (*ii*), lower mid; (*iii*), upper mid; (*iv*), upper end, including hook; each corresponds to the length of one face of an hepatocyte. The "hook" is a branch point, here the canaliculus dips into the liver and is lost from view. The large arrow points in the direction of bile flow (which is opposite to that of the sinusoidal micro-circulation, and towards the bile duct). Details of the contraction sequence is as follows: In *a*, note that i, ii, iii and iv segments are all patent and filled with fluorescein-labeled bile. In *b*, segments iii and iv have contracted (iii contracts first followed by iv, not shown) with extrusion of bile in the direction of the arrow and out of the field of vision. These segments are no longer visible because the fluoresceinated bile is no longer present. Segment i has also contracted; its fluorescence is lost. Segment ii shows increased fluorescence and is dilated; it has received bile from segment i. In *c*, note the return of fluorescence to segments ii, iii and iv (an appearance closely similar to that seen in *a*), this is ascribed to refilling of segments iii and iv from segment ii. Segment i is still contracted. *d–f* shows an almost identical contraction sequence. Bile flow is again in the direction of the arrow shown in *a*. *g–i* are close-up prints of *d–f*. (*S*), sinusoid. Bars; 10 μm.

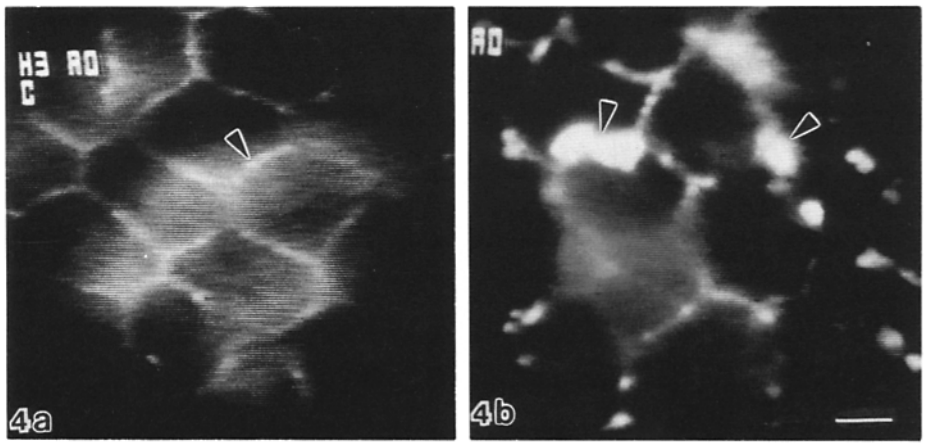

Figure 4. Fluorescent cinematomicrographs of the bile canalicular meshwork in vivo. (*a*) Control liver. A polygonal meshwork of the bile canalicular fluorescence (*arrowhead*) is uniformly recognized on the surface of the liver. (*b*) CB-infused liver. The bile canalicular fluorescence is irregularly and extensively dilated. Note the saccular dilatation of bile canaliculi (*arrowheads*). Bar, 10 μm.

dimensional network within the substance of the liver lobule were well visualized. They displayed a linear fluorescence pattern along the liver cell cords (Fig. 2, *e* and *f*). Short branches of linear bile canaliculi connected with a polygonal meshwork of bile canaliculi. Observing the same field by the transillumination method confirmed that this fluorescence corresponded to bile canaliculi.

The canalicular network remained patent for a variable length of time showing only nearly continuous fine fluctuations in caliber, but there were periods during which segments would become blacked out as they expelled a bolus of canalicular bile into a contiguous region of the network; these motions were interpreted as periodic contractions. After a variable time period, the canalicular fluorescence reappeared only to disappear again when the expulsive events would be repeated. These dynamic movements of bile canaliculi were recorded on time-lapse video. Bursts of canalicular activity were occasionally seen as depicted in

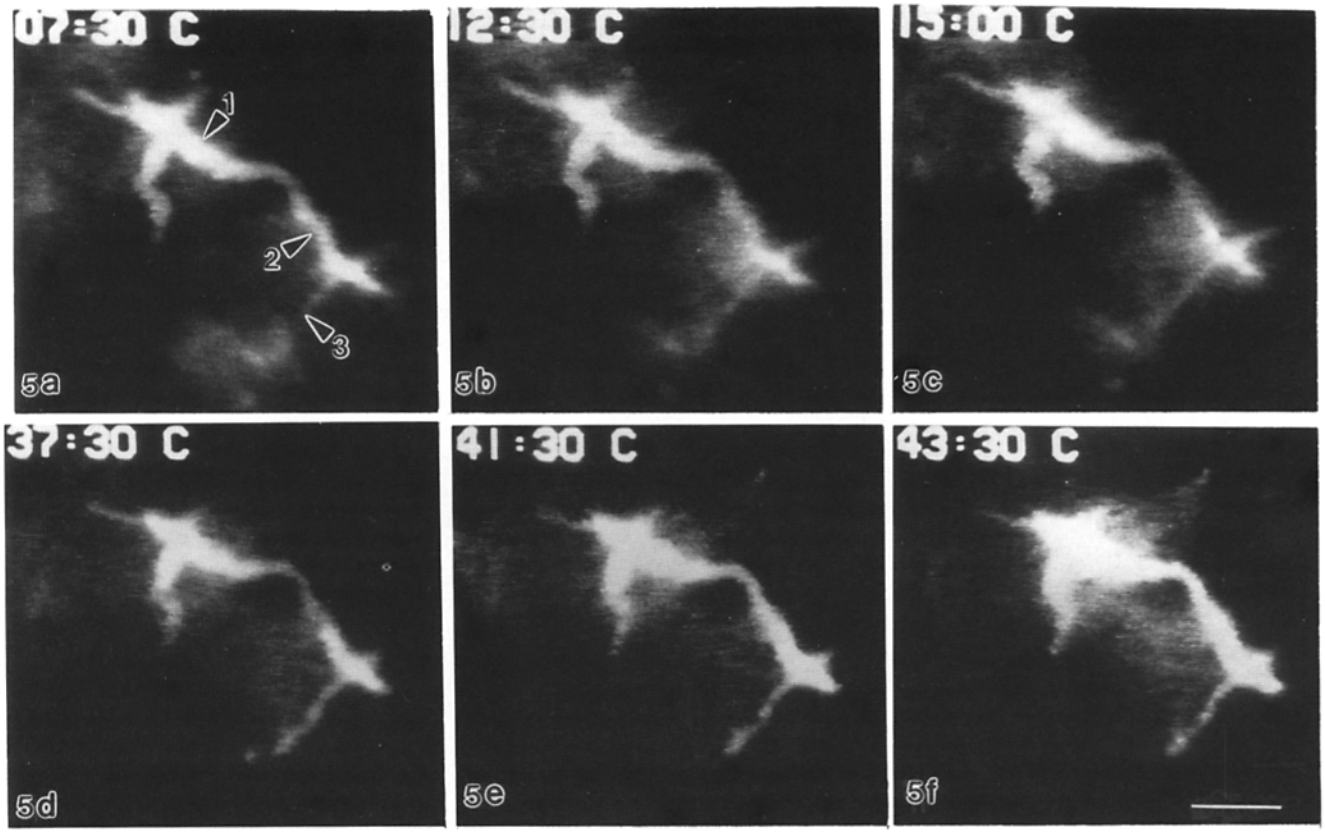

Figure 5. Fluorescent cinematomicrographs show the sequence of bile canalicular motility in vivo in CB-infused rats. Note that tubular distension of bile canaliculi shows impairment of canalicular motility. The real time in the upper left corner in each micrograph. The dilated region of bile canaliculi indicated by the arrowhead 1 is not changed for more than 30 min. In *e*, this region begins to dilate and dilates more and more in *f* with strong intensity of canalicular fluorescence. The region pointed by the arrowhead 2, shows extremely slow contraction in *b* and *c* and dilates again in *e* and *f*. The segment indicated by the arrowhead 3 continues to contract in *a*, *b*, and *c*, and dilates in *d*. The time represented by this sequence is 2,160 s (36 min). Bar, 10 μm.

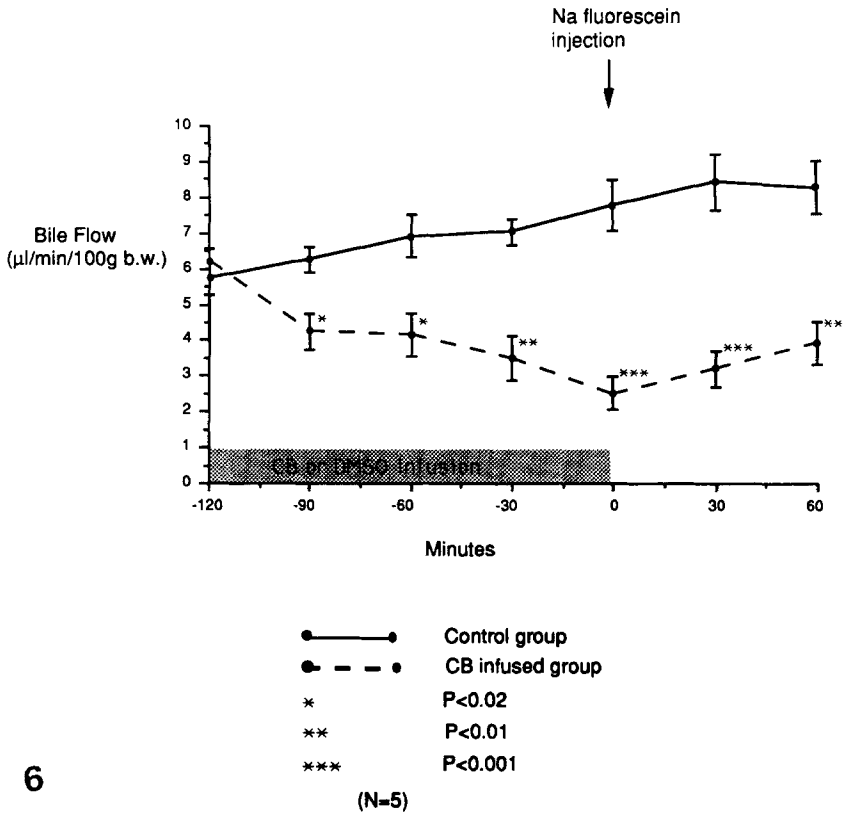

6

Figure 6. Effect of CB on bile flow. During the period of in vivo observation after injection of sodium fluorescein (time 0–60 min), bile flow with CB is significantly decreased. Note gradual return towards normal values suggesting reversibility of the CB effect.

Fig. 3. Bile canalicular contractions appeared to be forceful, expelling the fluorescein from one segment of the bile canalicular system to another. Variability in the completion of contractions in the same canalicular secretory unit is seen during a 38-s period in Fig. 3, *a–c* (17:13:41 → 17:14:19) and over 16 s in Fig. 3, *d–f* (17:18:15 → 17:18:31). The sequences always appeared unidirectional. The details of the contraction sequence is given in detail in Fig. 3. Not all segments demonstrated such motile behavior, suggesting that some regions are conductive or perhaps are resting rather than actively contractile. Movement of bile canaliculi appeared overall to be in a direction opposite to the liver's microcirculation which is in a portal to centrilobular direction. Bile canalicular contractions were most notable in zone 1 (periportal) regions; they were not observed in the subcapsular "chicken-wire" network of canaliculi on the liver surface. Great care was taken to ensure that the observed movements were not induced by changes of focus of the microscope or by movement of the liver itself; this was ascertained by using noncontractile reference points in the same field and by

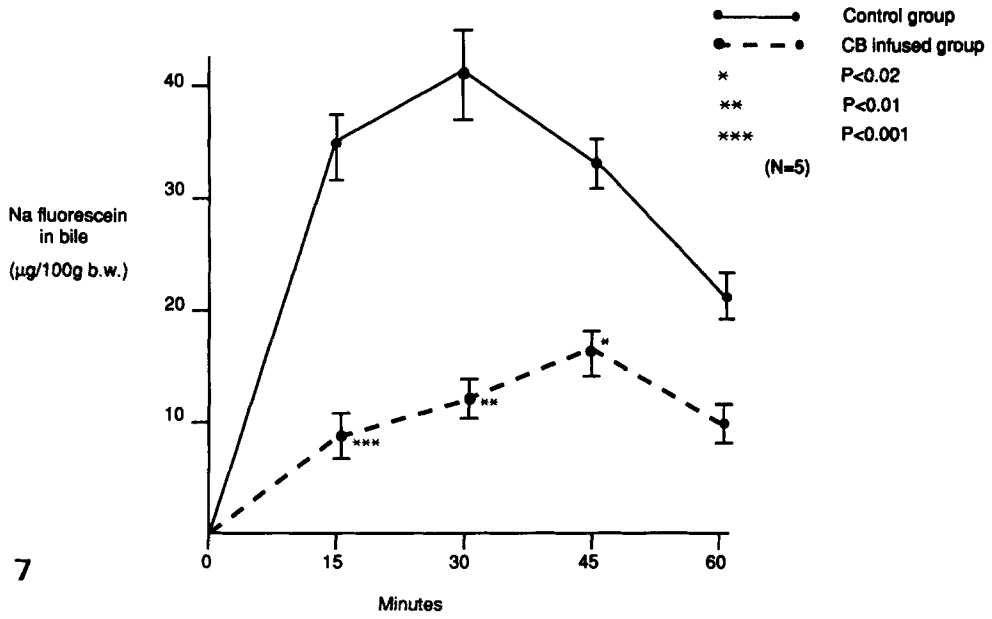

7

Figure 7. Biliary excretion of sodium fluorescein. The graph shows the amount of sodium fluorescein in the bile duct samples (volume of sample collected × concentration of sodium fluorescein). In controls, there is a short rise followed by a fall following the bolus injection. In the CB-treated group, there is a slow rise to a significantly low level and a delayed peak indicating impairment of bile flow.

deliberately focusing up and down periodically to ensure the focus was correct. Moreover, when a segment of canaliculus was in a closed or contracted state the fluorescence disappeared, and deliberately changing the plane of focus did not cause the segment to reappear.

Cytochalasin Infusion

As in normal liver, ~30 min after injection the fluorescence appeared in the bile canaliculi in both control and CB-infused groups. In the controls, a uniform polygonal meshwork of bile canalicular fluorescence was recognized on the surface of the liver (Fig. 4 *a*). However, in the CB-infused rats, bile canaliculi in acinar zone 1 became progressively dilated (Fig. 4 *b*). Saccular dilation of bile canaliculi was most noticeable at the branching points of the bile canalicular meshwork. In the control group, the diameter of bile canalicular fluorescence was 0.72 ± 0.03 μm (mean ± SEM, $n = 37$) and the minimum and maximum diameters were 0.41 and 1.16 μm. In the CB-infused group, the mean canalicular diameter increased to 1.83 ± 0.20 μm ($n = 10$) and the minimum and maximum diameters were 1.20 and 3.46 μm ($p < 0.005$). With CB, bile canaliculi were widened irregularly, and commonly this was extensive. Canalicular motility in the dilated areas, was impaired and contractile activity was reduced (Fig. 5). In addition, segments of the canalicular network displayed saccular or tubular distension with virtual cessation of canalicular motility. The distension progressed even after the removal of CB. In the saccular dilatations, the fluorescence was more intense than in surrounding canaliculi. The motile activity in areas of saccular distension was infrequent and extremely slow, and there were no contractions or loss of fluorescence. Dynamic and forceful movements of bile canaliculi observed in vivo in control liver (CB experiment) were identical to those found in normal liver. The microcirculation of the liver appeared normal in both controls and CB-infused rats.

Bile Flow

CB caused a diminution in bile flow and a delay in the appearance of sodium fluorescein in the bile. Bile flow, as assessed by measuring the bile collected in the bile duct cannula, was reduced by CB (Fig. 6). After the addition of CB, bile flow gradually decreased with time, and was significantly reduced (2.5 ± 0.5 μl/min/100 g b.w., $n = 5$) 2 h after CB as compared to controls (7.8 ± 0.7 μl/min/100 g b.w., $n = 5$) ($p < 0.001$). The time between injection and the appearance of sodium fluorescein in bile duct bile was significantly increased in CB-infused groups (220 ± 9 s, $n = 5$) compared to controls (83 ± 3 s, $n = 5$) ($p < 0.001$). The excretion of sodium fluorescein into bile duct bile was also altered by CB. In controls, sodium fluorescein appeared in the bile duct samples immediately after the injection via the mesenteric vein, and reached the maximum concentration 30 min after the injection of sodium fluorescein, subsequently disappearing from the bile quickly. In the CB-infused group, sodium fluorescein disappeared significantly later than in controls, and the excretion of sodium fluorescein was reduced (Fig. 7). In terms of liver function, the excretion of sodium fluorescein, as measured by bile duct collections, was significantly impaired by CB, confirming previous reports (40, 53). The effects depicted were after 2 h of CB infusion in a dosage that produces a potentially reversible injury (40). Despite the impairment of bile flow at the bile duct level, canalicular bile secretion apparently continues with CB administration (67).

The pH of bile was 8.70 in both the control and the CB-treated group. There was no fluctuation and no significant differences before or after injection with sodium fluorescein, hence it is unlikely that changes in pH are critical in this study.

EM

EM documented the nature of the bile canalicular changes observed in vivo. By scanning EM, marked bile canalicular dilation was noted mainly in zone 1 with CB (Fig. 8). As observed in vivo, there were two kinds of bile canalicular dilation, saccular and tubular. Saccular dilatation occurred mainly at the bifurcations in the bile canalicular meshwork. Transmission EM of the controls showed normal pericanalicular actin microfilamentous networks and actin cores in canalicular microvilli (Fig. 9 *a*). The livers of CB control rats were also normal, but in the CB-treated group, bile canaliculi were dilated, showed loss of microvilli, and had a granular rather than a filamentous ectoplasmic zone (Fig. 9 *b*).

Image Quantification

Changes in the IOD measurements of a canalicular segment reflect the degree of filling with fluorescence and hence the size or calibre of that segment. The values of IOD, which represent a relative measurement, were constantly changing (Fig. 10). At times, an increase in the luminal diameter of one segment was associated with a decrease in the luminal diameter of an adjacent segment. There appeared to be coordination of contraction and dilatation, with emptying of one segment associated with filling of the next segment (e.g., time 190–235 s in Fig. 10). The video sequence has suggested a unidirectional pattern of flow, although such a phenomenon could not be evaluated by IOD measurements. The length of time required for the canaliculi to empty was variable, but at times was 15 s or less.

Discussion

Dynamic contractile movements of bile canaliculi were observed in the normal rat in vivo, but the motile activity was inhibited or abolished by cytochalasin B. These results have important implications for liver structure and function with respect to mechanisms of bile secretion and flow. The contractions appear functional since they have an active pumping action with movement of canalicular bile from contractile to conducting regions of the canalicular system. Their functional role in bile flow is exemplified further by the alterations seen with CB since impairment of canalicular motility leads to intrahepatic canalicular cholestasis.

There may be two routes of bile filling of canaliculi in vivo. One is the active secretion of bile by the contiguous hepatocytes which compose any individual segment of the bile canaliculus (47). Secondly, bile may come from the upstream regions of the bile canalicular system which is an open network of channels.

The general overall direction of bile flow in the liver lobule is from zone 3 (central) to zone 1 (periportal) and from there into the portal bile ducts which drain into the interlobular

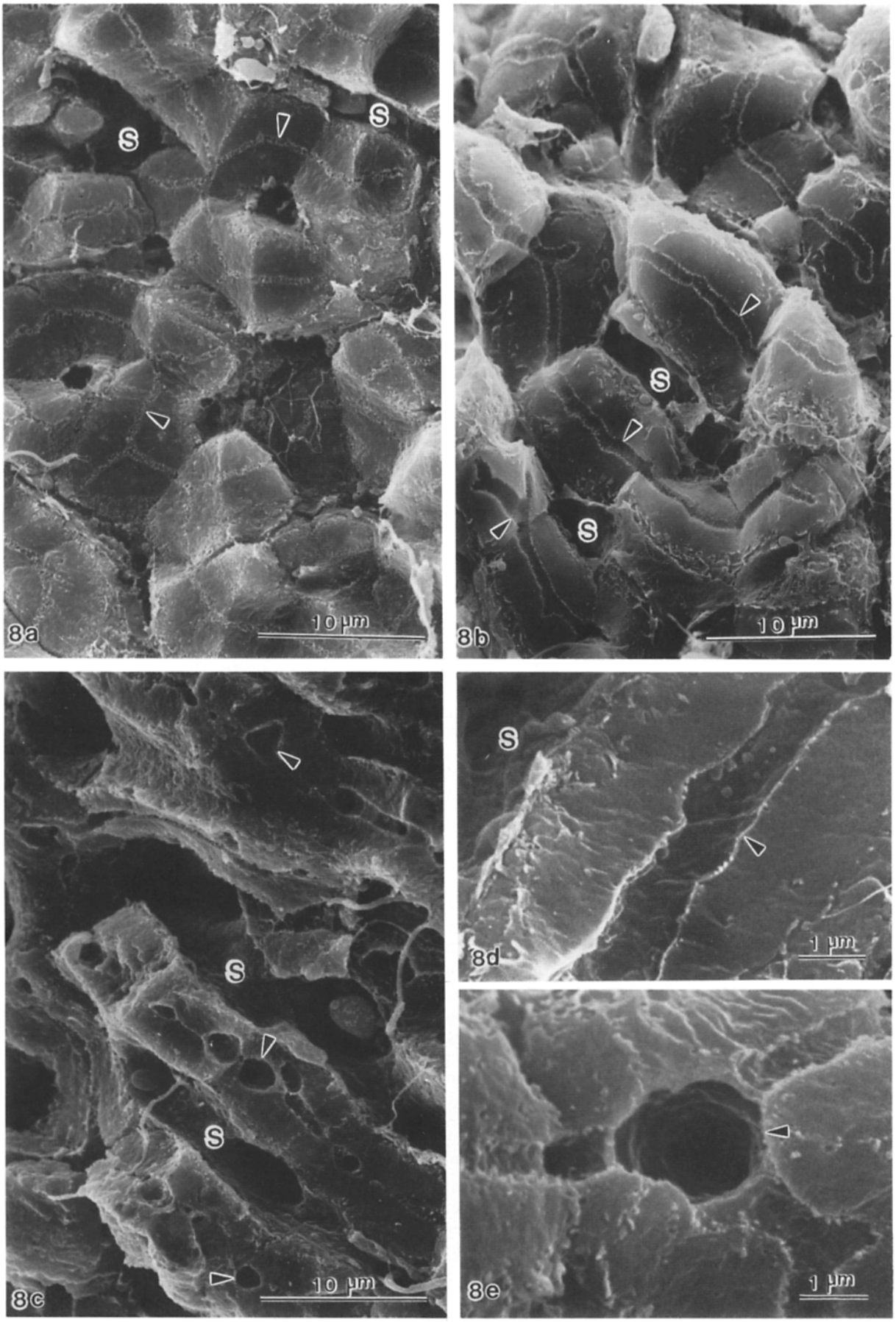
S
S
10 μm
8a
S
S
10 μm
8b
S
S
10 μm
8c
S
1 μm
8d
1 μm
8e

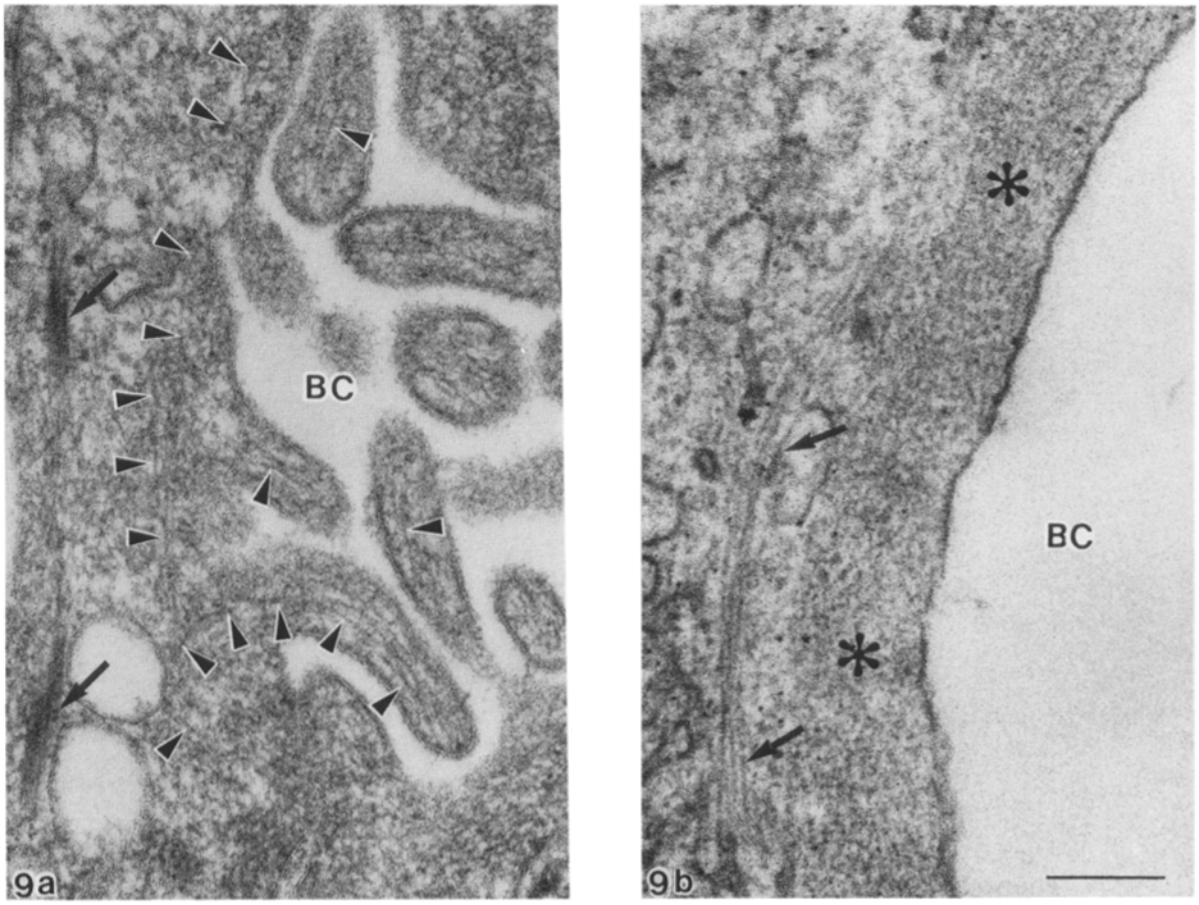

Figure 9. Transmission electron micrographs of rat liver. (*a*) Control liver. Portion of bile canaliculus (*BC*). Actin filaments (*arrowheads*) are noted in microvilli and form a network around the canaliculus. Intermediate filaments (*arrows*) in bundles are also seen. Uranyl acetate and lead citrate stain. (*b*) CB-infused liver. Part of a dilated bile canaliculus (*BC*) is shown. Note the loss of microvilli and ectoplasmic thickening (*asterisks*). The actin microfilamentous zone is granular in appearance (compare with *a*). Intermediate filaments (*arrows*) are again seen. Uranyl acetate and lead citrate stain. Bar, 0.1 μm.

and main hepatic ducts. While the video sequences suggested that flow was unidirectional (as indicated by the arrow in Fig. 3), such dynamic events cannot be readily demonstrated by static images. IOD measurements of unidirectional flow would be characterized by sequential contractions of the lower, middle and upper segments (Fig. 10). Such an observation could not be made with certainty because of the limits of the microscopic methods and quantitation techniques.

The almost continuous fine fluctuations in caliber are perhaps related to maintaining tone and may reflect the elasticity of the canalicular membrane, and are not regarded as contractions. With regard to contractions per se, not all components of the bile canalicular network exhibited equal contractile activity. For instance, the "chicken-wire" network of canaliculi present on the surface of the liver (subcapsular) showed no contractions. Contractions were most frequently observed in zone 1 (periportal) canaliculi. This is especially interesting since bile acid secretion is predominantly a function of zone 1 hepatocytes (8, 22, 41). It is of special interest that the effects of CB were also most marked in zone 1, which would be expected if the functional basis of canalicular contraction is actin filament mediated. Not only were contractions greatly impaired by CB, but canalicular walls which are normally supported by actin, appeared weakened and became overdistended to the point of sacculation. Bile canalicular sacculations have also been reported in the rat treated with alpha-naphthyl isothiocyanate (6). The observation that

Figure 8. Scanning electron micrographs of a fractured surface of rat livers. (*a*) Control liver. Note the chicken wire-like anastomosing network of bile canaliculi (*arrowheads*). Canalicular lumina are uniformly filled with microvilli. (*S*), sinusoid. (*b*) CB-infused liver. Note the marked tubular dilatation of bile canaliculi (*arrowheads*). (*c*) CB-infused liver. Bile canaliculi are extensively dilated. Note the saccular dilatation of bile canaliculi (*arrowheads*). (*d*) High magnification of the tubular dilatation of bile canaliculi in CB-infused livers. Note the complete loss of canalicular microvilli and the greatly dilated canalicular lumen (*arrowhead*). (*e*) High magnification of the saccular dilatation of bile canaliculi in CB-infused livers. Mainly at the bifurcation of the canalicular system, bile canaliculi are saccularly dilated with loss of microvilli (*arrowhead*).

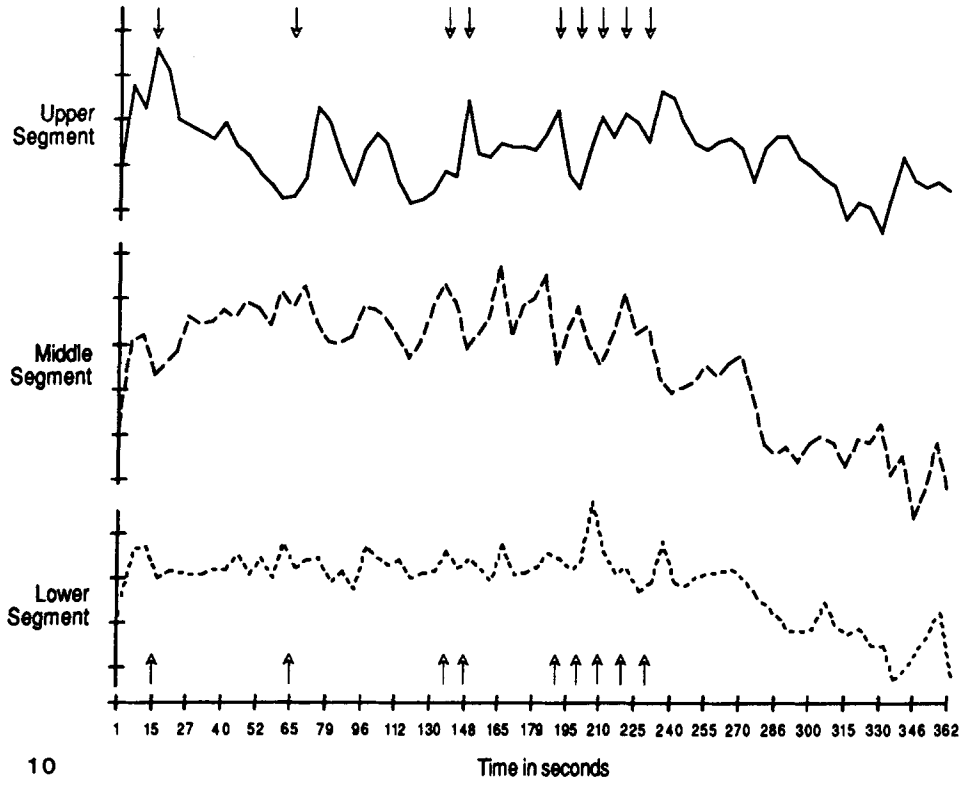

Figure 10. IOD measurements, taken from three adjacent segments of bile canaliculi similar to that shown in Fig. 3. The vertical scale represents the intensity of fluorescence within canalicular lumina, and hence the size of the canaliculi. Arrows demonstrate those times when a diminution in fluorescence of one segment (interpreted as contraction) was associated with an increase in fluorescence (dilation) of a neighboring segment. During some contractions of the middle and upper segment, the lower segment appears to have remained isometric (e.g., times 15 and 65). At other times (e.g., 206 and 235), contraction of the lower segment was associated with dilatation of the middle segment. In the case of the middle and upper segments, there is a "saw-tooth" type pattern with a tendency for a decrease in intensity of the middle segment to be followed almost immediately by an increase in fluorescence of the upper segment (e.g., scale points 15, 65, 140, 148, and 190–235). This pattern fits best with the sequences seen in the movie and with the images depicted in Fig. 3. The apparent lack of synchrony at other time points is not because of retrograde filling, since the upper segment empties into the next adjacent segment (not shown); the presence of branch points and the limitations of the method are the likely explanation. In the region where there is a burst of canalicular contractions (179–240 s) the time interval between contractions is in the 20–40 s range. At other times it is more variable. Notice that in the last 60–90 s of this 6-min video sequence, there appears to be diminution in the intensity of fluorescence within the canaliculi; this could represent a physiological change or it may have resulted from artefactual extinguishing of the fluorescence by UV illumination.

the sacculations appeared first at branch points of canaliculi suggests special sensitivity, or function of actin filaments in these regions.

In neither CB-treated animals nor in the controls was there evidence of leakage of fluorescent material between the cells (paracellular pathway of bile secretion) (21). This is an important difference from isolated liver cell couplets in which emptying of canalicular lumina is accompanied by passage of canalicular bile between the cells through tight junctions which are presumably leaky (52, 55). The in vivo phenomenon of dynamic, pumping motions that visibly propel bile along the canaliculus would be inconsistent with the rupture and collapse theory of canalicular motion that has been applied to liver cell couplets (9, 10, 30, 35). Hence, while "collapses" may occur in isolated hepatocyte couplets, this is not seen in vivo.

These in vivo results using normal and CB-treated rats add significant weight to the concept that bile canalicular motility is an active, dynamic process in the normal liver, where it likely facilitates canalicular bile flow (52). The results of these in vivo studies can be compared to previous in vitro investigations using isolated hepatocyte couplets (55, 62). In both, canalicular contractions follow the same general pattern, the degree of canalicular emptying was variable, as were the lengths of time required for the dilatation phase (canalicular filling) and contractile phase. Also, in both, random appearing partial or complete contractions occurred at variable time intervals interrupted by bursts of contractile activity in which the contraction interval is much shorter. However, canalicular contractions in vivo are capable of a 10-fold increase in contraction rate compared to that seen in isolated couplets. For instance, in bursts of activity, the time interval between contractions was 300–360 s in couplets (55) and 20–40 s in vivo (Fig. 3). It must be remembered however, that bile canalicular contractions are closely linked to bile flow and that in vivo, bile can reach an individual canaliculus from dual sources, that secreted and that coming from contiguous canaliculi; in contrast, in the isolated couplet, the only bile present is that secreted by the couplet cells themselves; this could explain an order of magnitude difference in the contraction rate.

In previous in vivo studies, it has been difficult to obtain both satisfactory resolution and to record fluorescence images for more than a few seconds because of fading of the fluorescence and because of photooxidation-induced damage to living cells. These problems have have resolved by advances in technology which permit very low levels of illumination and enhancement of video images by real-time processing, to visualize what would otherwise be indefinite, blurred, or simply invisible (31). Further, this study exemplifies the usefulness of this technology (36, 38) in the examination of in vivo functions at the tissue and organ level, per-

mitting correlation of subcellular events with structural and functional changes in the living organism.

The authors thank Mr. Vernon Edwards, Mrs. Janet Rowley, Mr. Jim Portman, Mr. Michael Starr, and Mr. Cameron Ackerley for excellent technical assistance.

This research was supported by grants-in-aid of the Medical Research Council of Canada (MRC MT-0785) and Equipment Grant (MRC Me-8215). The authors thank Dr. Sergio Grinstein, Head, Division of Cell Biology, Research Institute, The Hospital for Sick Children for reading this manuscript and for providing helpful comments.

Received for publication 28 September 1991 and in revised form 10 February 1991.

References

1. Adelstein, R. S. 1982. Calmodulin and the regulation of the actin-myosin interaction in smooth muscle and nonmuscle cells. *Cell.* 30:349–350.
2. Allen, R. D. 1985. New observations on cell architecture and dynamics by video-enhanced contrast optical microscopy. *Annu. Rev. Biophys. Chem.* 14:265–290.
3. Allen, R. D., N. S. Allen, and J. L. Travis. 1981. Video-enhanced contrast, differential interference contrast (AVEC-DIC) microscopy: a new method capable of analyzing microtubule-related motility in the reticulopodial network of allogromia laticollaris. *Cell. Motil.* 1:291–302.
4. Allen, R. D., J. L. Travis, N. S. Allen, and H. Yilmaz. 1981. Video-enhanced contrast polarization (AVEC-POL) microscopy: a new method applied to the detection of birefringence in the motile reticulopodial network of allogromia laticollaris. *Cell. Motil.* 1:275–289.
5. Barth, C. A., and L. R. Schwarz. 1982. Transcellular transport of fluorescein in hepatocyte monolayers: evidence for functional polarity of cells in culture. *Proc. Natl. Acad. Sci. USA.* 79:4985–4987.
6. Bhathal, P. S., and G. S. Christie. 1969. A fluorescence microscopic study of bile duct proliferation induced in guinea pigs by alpha-naphthyl isothiocyanate. *Lab. Invest.* 20:480–487.
7. Bhathal, P. S., and G. S. Christie. 1969. Intravital fluorescence microscopy of the terminal and subterminal portions of the biliary tree of normal guinea pigs and rats. *Lab. Invest.* 20:472–479.
8. Boyer, J. L. 1980. New concepts of mechanisms of hepatocyte bile formation. *Physiol. Rev.* 60:303–325.
9. Boyer, J. L. 1987. Contractile activity of bile canaliculi: contraction or collapse? *Hepatology.* 7:190–192.
10. Boyer, J. L., A. Gautam, and J. Graf. 1988. Mechanisms of bile secretion: insights from the isolated rat hepatocyte couplet. *Sem. Liver Dis.* 8:308–316.
11. Boyles, J. 1984. The use of primary amines to improve glutaraldehyde fixation. *In* The Science of Biological Specimens for Electron Microscopy and Microanalysis. Revel, J. P., T. Barnard, and G. H. Haggis, editors. Scanning Microscopy International, Chicago, IL. 7–21.
12. Brenner, S. L., and E. D. Korn. 1979. Substoichiometric concentration of cytochalasin D inhibit actin polymerization: additional evidence for an F-actin treadmill. *J. Biol. Chem.* 254:9982–9985.
13. Broschat, K. O., R. P. Stidwill, and D. R. Burgess. 1983. Phosphorylation controls brush border motility by regulating myosin structure and association with the cytoskeleton. *Cell.* 35:561–571.
14. Brown, S. S., and J. A. Spudich. 1979. Cytochalasin inhibits the rate of elongation of actin filament fragments. *J. Cell Biol.* 83:657–662.
15. Brown, S. S., and J. A. Spudich. 1981. Mechanism of action by cytochalasin: evidence that it binds to actin filament ends. *J. Cell Biol.* 88:487–491.
16. Cerny, L. C., and E. Bandman. 1986. Contractile activity is required for the expression of neonatal myosin heavy chain in embryonic chick pectoral muscle cultures. *J. Cell Biol.* 103:2153–2161.
17. Cooper, J. A. 1987. Effects of cytochalasin and phalloidin on actin. *J. Cell Biol.* 105:1473–1478.
18. Craig, R., R. Smith, and J. Kendrick-Jones. 1983. Light-chain phosphorylation controls the conformation of vertebrate non-muscle and smooth muscle myosin molecules. *Nature (Lond.)* 302:436–439.
19. Dollery, C. T., J. V. Hodge, and M. Engel. 1962. Studies of the retinal circulation with fluorescein. *Br. Med. J.* 2:1210–1215.
20. Dubin, M., M. Maurice, G. Feldman, and S. Erlinger. 1978. Phalloidin-induced cholestasis in the rat. *Gastroenterology.* 75:450–455.
21. Elias, E., Z. Hruban, J. B. Wade, and J. L. Boyer. 1980. Phalloidin-induced cholestasis. A microfilament-mediated change in junctional complex permeability. *Proc. Natl. Acad. Sci. USA.* 77:2229–2233.
22. Erlinger, S. 1988. Bile Flow. *In* The Liver: Biological Pathobiology. Second Edition. Arias, I. M., W. B. Jakoby, H. Popper, D. Schachter, and D. A. Shafritz, editors. 643–661. Raven Press, New York.
23. Exton, J. 1988. Role of phosphoinositides in the regulation of liver function. *Hepatology.* 8:152–166.
24. Fernandez, A., L. Brautigan, M. Mumby, and N. J. C. Lamb. 1990. Protein phosphatase type 1 but not type 2A, modulates actin microfilament integrity and myosin light chain phosphorylation in living non muscle cells. *J. Cell Biol.* 111:103–112.
25. Flanagan, M. D., and S. Lin. 1980. Cytochalasin block actin filament elongation by binding to high affinity sites associated with F-actin. *J. Biol. Chem.* 255:835–838.
26. Foskett, J. K. 1988. Simultaneous Nomarski and fluorescence imaging during video microscopy of cells. *Am. J. Physiol.* 255:C566–C571.
27. Foskett, J. K., P. J. Gunter-Smith, J. E. Melvin, and R. J. Turner. 1989. Physiological localization of an agonist-sensitive pool of Ca^{2+} in parotid acinar cells. *Proc. Natl. Acad. Sci. USA.* 86:167–171.
28. French, S. W., and P. L. Davies. 1975. Ultrastructural localization of actin-like filaments in rat hepatocytes. *Gastroenterology.* 68:765–774.
29. Gabbiani, G., R. Montesano, R. Tuchweber, M. Salas, and L. Orci. 1975. Phalloidin-induced hyperplasia of actin filaments in rat hepatocytes. *Lab. Invest.* 33:562–569.
30. Gautam, A., O. C. Ng, and J. L. Boyer. 1987. Isolated rat hepatocyte couplets in short term culture-structural characteristics and plasma membrane reorganization. *Hepatology.* 7:216–233.
31. Gebhardt, R., and W. Jung. 1982. Biliary secretion of sodium fluorescein in primary monolayer cultures of adult rat hepatocytes and its stimulation by nicotinamide. *J. Cell Sci.* 56:233–244.
32. Goddette, D. W., and C. Frieden. 1985. The binding of cytochalasin D to monomeric actin. *Biochem. Biophys. Res. Commun.* 128:1087–1092.
33. Gordon, D. L., J. L. Boyer, and E. D. Korn. 1977. Comparative biochemistry of non-muscle actin. *J. Biol. Chem.* 252:8300–8309.
34. Govindan, V. M., and T. H. Wieland. 1975. Isolation and identification of an actin from rat liver. *FEBS (Fed. Eur. Biochem. Soc.) Lett.* 59:117–119.
35. Graf, J., and J. L. Boyer. 1990. The use of isolated rat hepatocyte couplets in hepatobiliary physiology. *J. Hepatol.* 10:387–394.
36. Hanzon, V. 1952. Liver cell secretion under normal and pathologic conditions studied by fluorescence microscopy on living rats. *Acta. Physiol. Scand.* 28(Suppl. 101):1-268.
37. Hartwig, J. H., and T. P. Stosell. 1979. Cytochalasin B and the structure of actin gels. *J. Mol. Biol.* 134:539–553.
38. Hayden, J. H., and R. D. Allen. 1984. Detection of single microtubules in living cells: particle transport can occur in both directions along the same microtubule. *J. Cell Biol.* 99:1785–1793.
39. Holborow, E. J., P. S. Trenchev, J. Dorling, and J. Webb. 1975. Demonstration of smooth muscle contractile protein antigens in liver and epithelial cells. *Ann. NY Acad. Sci.* 254:489–504.
40. Jahn, W. 1973. Similarity between the effects of experimental congestion of the isolated perfused rat liver and the action of cytochalasin B. *Naunyn Schmiedebergs Arch. Pharmacol.* 278:431–434.
41. Jones, A. L., D. L. Schmuckler, R. H. Renston, and T. Murakami. 1980. The architecture of bile secretion. A morphological perspective of physiology. *Dig. Dis. Sci.* 25:609–628.
42. Korn, E. D. 1982. Actin polymerization and its regulation by proteins from non-muscle cells. *Physiol. Rev.* 62:672–737.
43. Lamb, N. J. C., A. Fernandez, M. A. Conti, R. Adelstein, D. B. Glass, W. J. Welch, and J. Fermisco. 1988. Regulation of actin microfilament integrity in living nonmuscle cells by the cAMP-dependent protein kinase and the myosin light-chain kinase. *J. Cell Biol.* 106:1955–1971.
44. Lin, D. C., and S. Lin. 1979. Actin polymerization induced by a motility-related high-affinity cytochalasin binding complex from human erythrocyte membranes. *Proc. Natl. Acad. Sci. USA.* 76:2345–2349.
45. Lin, D. C., K. D. Tobin, M. Grumet, and S. Lin. 1980. Cytochalasins inhibit nuclei-induced actin polymerization by blocking filament elongation. *J. Cell Biol.* 84:455–460.
46. McLean-Fletcher, S., and T. D. Pollard. 1980. Mechanism of action of cytochalasin B on actin. *Cell.* 20:329–341.
47. Miyairi, M., C. Oshio, S. Watanabe, C. R. Smith, I. M. Yousef, and M. J. Philips. 1984. Taurocholate accelerates bile canalicular contractions in isolated rat hepatocytes. *Gastroenterology.* 87:788–792.
48. Mizel, S. B., and L. Wilson. 1972. Inhibition of the transport of several hexoses in mammalian cells by cytochalasin B. *J. Biol. Chem.* 245: 4102–4105.
49. Oda, M., and M. J. Phillips. 1977. Bile canalicular membrane pathology in cytochalasin B-induced cholestasis. *Lab. Invest.* 37:350–356.
50. Oda, M., V. M. Price, M. M. Fisher, and M. J. Phillips. 1974. Ultrastructure of bile canaliculi with special reference to the surface coat and the pericanalicular web. *Lab. Invest.* 31:314–323.
51. Oda, M., M. Nakamura, N. Watanabe, Y. Ohya, E. Sekizuka, N. Tsukada, Y. Yonei, H. Komatsu, H. Nagata, and M. Tsuchiya. 1983. Some dynamic aspects of the hepatic microcirculation-demonstration of sinusoidal endothelial fenestrae as a possible regulatory factor. *In* Intravital observation of organ microcirculation. Tsuchiya, M., H. Wayland, M. Oda, and I. Okazaki, editors. 105–138. Excerpta Medica, Amsterdam, Netherlands.
52. Oshio, C., and M. J. Phillips. 1981. Contractility of bile canaliculi, implications for bile flow. *Science (Wash. DC).* 212:1041–1042.
53. Phillips, M. J., M. Oda, E. Mak, M. M. Fisher, and K. N. Jeejeebhoy. 1975. Microfilament dysfunction as a possible cause of intrahepatic cholestasis. *Gastroenterology.* 69:48–58.

54. Phillips, M. J., M. Oda, I. M. Yousef, and K. Funatsu. 1981. Effects of cytochalasin B on membrane-associated microfilaments in a cell-free system. *J. Cell Biol.* 91:524–527.
55. Phillips, M. J., C. Oshio, M. Miyairi, H. Katz, and C. R. Smith. 1982. A study of the canalicular contractions in isolated hepatocytes. *Hepatology.* 2:763–768.
56. Pollard, T. D., and J. A. Cooper. 1986. Actin and actin-binding proteins. A critical evaluation of mechanisms and functions. *Annu. Rev. Biochem.* 55:987–1035.
57. Rampal, A. L., H. B. Pinkofsky, and C. Y. Jung. 1980. Structure of cytochalasins and cytochalasin B binding site in human erythrocyte membranes. *Biochemistry.* 19:679–683.
58. Sato, T. 1968. A modification method for lead staining of thin sections. *J. Electron Micros.* 17:173–180.
59. Schliwa, M. 1981. Proteins associated with cytoplasmic actin. *Cell.* 25:587–590.
60. Schliwa, M. 1982. Action of cytochalasin D on cytoskeletal networks. *J. Cell Biol.* 92:79–91.
61. Sellers, J. R., and R. S. Adelstein. 1987. Regulation of contractile activity. *Enzymes.* 18:381–418.
62. Smith, C. R., C. Oshio, M. Miyairi, M. Katz, and M. J. Phillips. 1985. Coordination of the contractile activity of bile canaliculi. *Lab. Invest.* 53:270–274.
63. Tanenbaum, S. W. 1978. Cytochalasins, biochemical and cell biological aspects. *In* Frontiers of Biology Series. Nauberger, A., and E. L. Tatum, editors. North-Holland Publishing Co., Amsterdam, Netherlands.
64. Tilney, L. G., Y. Fukui, and D. J. DeRosier. 1987. Movement of the actin filament bundle in Mytilus sperm: A new mechanism is proposed. *J. Cell Biol.* 104:981–993.
65. Warrick, H. M., and J. A. Spudich. 1987. Myosin structure of motion in cell motility. *Annu. Rev. Cell Biol.* 3:379–421.
66. Watanabe, S., and M. J. Phillips. 1984. Ca^{2+} causes active contraction of bile canaliculi: direct evidence from microinjection studies. *Proc. Natl. Acad. Sci. USA.* 81:6164–6168.
67. Watanabe, S., M. Tomono, M. Hirose, M. Takeuchi, T. Kitamura, and T. Namihisa. 1987. Microscopic fluorometric analysis of Na-fluorescein transport in the smallest secretory unit (couplet hepatocytes) and the effects of cytochalasin B. *Lab. Invest.* 56:146–150.
68. Weihing, R. R. 1976. Cytochalasin B inhibits actin-related gelation of HeLa cell extracts. *J. Cell Biol.* 71:303–307.
69. Wessels, N. K., B. S. Spooner, J. F. Ash, M. O. Bradley, M. A. Luduena, E. L. Taylor, J. T. Wrenn, and K. M. Yamada. 1971. Microfilaments in cellular and developmental processes. *Science (Wash. DC).* 171:1135–1143.